International Journal of Innovative
Computing, Information and Control
Volume **15**, Number **3**, June **2019**

ICIC International ©2019 ISSN 1349-4198
pp. 905–921

DETECTION OF SURFACE FLAWS ON TEXTURED LED LENSES USING WAVELET PACKET TRANSFORM BASED PARTIAL LEAST SQUARES TECHNIQUES

Hong-Dar Lin and Hsing-Lun Chen

Department of Industrial Engineering and Management
Chaoyang University of Technology
168, Jifong E. Road, Wufong District, Taichung 41349, Taiwan
hdlin@cyut.edu.tw

Received July 2018; revised November 2018

Abstract. *Light-emitting diode (LED) lenses, one kind of optical components, are popular and widely used in digital cameras, cell phones, and CD-ROMs. Nevertheless, a LED lens with a textured and uneven surface is more difficult to detect the visual defects than electronic components by current computer vision systems. This research proposes a wavelet packet transformation (WPT) based partial least squares (PLS) approach, called WPLS, to detect visual defects of LED lenses with structural textures. Three steps are developed to finish the process of defect detection. We first convert a spatial domain image to the WPT domain and extract the wavelet features of the sub-band images. Subsequently, the proposed PLS method is applied to multivariate transform and data reduction with wavelet features to obtaining latent images. Last, the latent images are fitted by a regression model to produce a predicted image and then subtract with the original image to get the residual image where the visual defects have been separated. Therefore, the intricate flaws on textured and uneven surfaces are precisely identified by the suggested scheme. The experimental results show that the proposed approach detects surface flaws more precisely than the conventional methods. Moreover, regarding the performance comparisons of the wavelet packet based multivariate techniques in defect detection of the textured LED lenses, the proposed WPLS method outperforms the other techniques, the WPT based principal component analysis (WPCA) method and the WPT based back propagation network (WBPN) model.*

Keywords: Industrial inspection, LED lens, Computer vision system, Wavelet packet transform, Partial least squares, Multivariate techniques

1. **Introduction.** A lens is an optical device with perfect or approximate axial symmetry which transmits and refracts light, converging or diverging the beam. Lenses are typically made of glass or transparent plastic. Optical lenses are transparent components made from optical-quality materials and curved to converge or diverge transmitted rays from an object. These rays then form a real or virtual image of the object. There are many types of optical lenses. Optical lenses are widely used in cell phone, notebooks, automotive, digital camera, LED, etc.

A light-emitting diode (LED) is a semiconductor device that emits visible light when an electric current passes through the semiconductor chip. Compared with incandescent and fluorescent illuminating devices, LEDs have lower power requirement, higher efficiency, and longer lifetime. Typical applications of LED components include indicator lights, LCD panel backlighting, fiber optic data transmission, etc. The functions of LED lenses include focusing, beauty, and protection to avoid the waste of light and light pollution.

DOI: 10.24507/ijicic.15.03.905

An LED without the assistance of lens focus function cannot project light to far distance. Therefore, LED lenses are invented to improve the light scattering problems of LEDs and they are widely applied to hand flashlights and traffic lights applications. Appearance differences among the clear lenses, diffused lenses, and textured lenses of LEDs are various designs for providing the lighting energy distribution in the areas of interest and reducing the uncomfortable glare effect for the general illumination applications. Figure 1 shows regular LEDs with clear lens, diffused lens, and textured lens. The structure of textured LED lenses with coarse and uneven surfaces is significantly different from those of the clear lenses and diffused lenses.

FIGURE 1. LED lenses with clear, diffused, and textured surfaces

To meet consumer and industry needs, LED products are being made in smaller sizes, which increase difficulties of product inspection. Lens inspection requires special physical conditions, particularly in terms of lighting. In the real working situation, each inspected lens is brought into the inspector's field of vision. The lenses are round and textured and the visual defects to be inspected could be located on the external surfaces of the lenses or inside. The textured lens has the appearance of periodic small circles in spatial domain image which is more complicated than those of the clear lens and diffused lens. It is more difficult to accurately detect visual defects embedded in the complicated structural textures. The majority of defects are not only very small but also they are extremely diverse and can assume various forms. Figure 2 shows a normal textured LED lens and two lenses with various shapes and low contrast of visual defects on uneven surfaces.

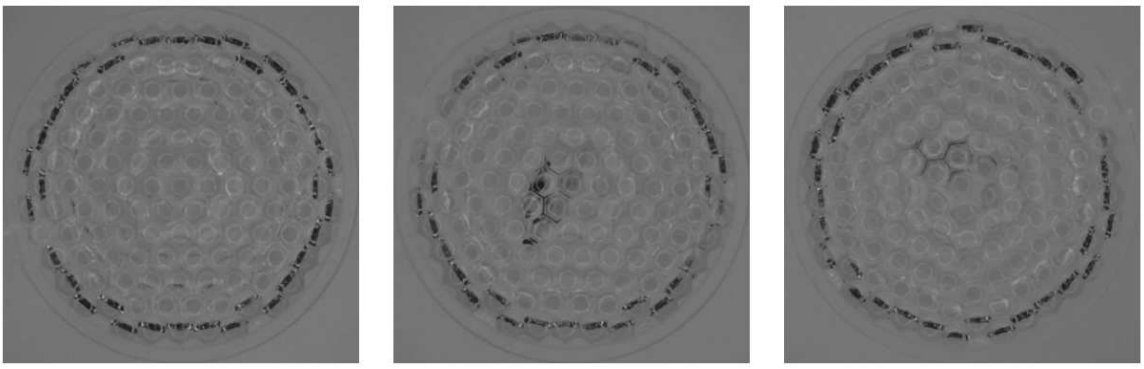

FIGURE 2. A normal textured LED lens and two lenses with various low contrast defects

Currently, the most common detection method for visual defects on LED lenses is human visual inspection. Human visual inspection is tedious, time-consuming and highly dependent on the inspectors' experiences, conditions, or moods. Erroneous judgments are easily made because of inspectors' subjectivity and eye fatigues. Difficulties exist in correctly inspecting intricate flaws by machine vision systems because when product

images are being captured, the area of an intricate flaw could expand, shrink or even disappear due to uneven illumination of the environment, texture structures and uneven surfaces of the products, and so on. Since the textured LED lens has the appearance of repeated small circles, those apparent textures make the flaw detection task harder when visual flaws are inlaid on the uneven surfaces of structural textures. We thereby propose a wavelet packet transformation (WPT) based partial least squares (PLS) approach, called WPLS, to conquer these problems of automated surface flaw inspection of LED lenses.

The WPT has the advantages of being fine enough to extract necessary information from the decomposed components and representing generalization of multi-resolution decomposition. The PLS regression is a modern method that integrates features from principal component analysis and multiple regression. Such advantages of WPT and PLS make WPLS approach suitable and favorable for our study of visual flaw detection of textured LED lenses with uneven surfaces.

The rest of the paper is organized as follows. First, we review the literature on optical techniques of computer vision for flaw detection. Second, we explain the proposed image models for inspecting surface flaws on textured LED lenses. Third, we conduct the experiments and evaluate the performance of the proposed models with known methods. Fourth, we present the conclusion and the future work.

2. **Literature Review.** Automated inspection of surface flaws has become a crucial mission for industries who exert to upgrade product quality and manufacturing efficiency [1,2]. Flaw inspection technologies are ordinarily classified into spatial domain and frequency domain approaches. In spatial domain techniques, Lin and Hsieh [3] developed a novel vision system based on slight deviation control techniques to detect surface variations on curved mirrors of vehicles. Adamo et al. [4] proposed a low-cost inspection system based on the Canny edge detection for online defects assessment in satin glass. In frequency domain technologies, Liu et al. [5] presented the watershed transform based methods to segment the possible defective regions and extract features of bottle wall by rules. Lin and Ho [6] suggested a global approach that applies discrete cosine transform-based enhancement for the automatic inspection of pinhole defects in randomly textured surfaces of capacitor chips of passive components. Li and Tsai [7] introduced a wavelet-based discriminant measure for defect inspection in multi-crystalline solar wafer images with inhomogeneous texture.

Some studies investigated the flaw inspection of LED related products. Lin and Jiang [8] developed a machine vision system that applies block discrete cosine transform and grey relational analysis for the automated visual inspection of tiny flaws occurring in the domed surfaces of LED epoxy-packing. Chiu and Lin [9] applied block discrete cosine transform, Hotelling's T-squared statistic, and grey clustering technique for the automated detection of surface flaws on LEDs with clear lenses. As to inspecting defects of lenses, Rebsamen et al. [10] described quality control procedures in the optical industry from a work analysis of optical lens inspection to a training program. Martínez et al. [11] developed a vision sensor planning system for automated inspection of headlamp lenses. This system integrated a vision sensor model and the customer requirements described by a fuzzy approach to achieve an optimal set of viewpoints by genetic algorithm. Bazin et al. [12] presented an optical technique for industrial inspection of ophthalmic contact lenses in a time constrained production line environment. Perng et al. [13] suggested a new inspection system that uses machine vision to detect optical defects in quasi-contact lenses.

From the above review of literature, it is evident that many of the lens related works focus on the distortion detection of optical lenses. Therefore, most of the current studies

pay attention to inspections of LED lenses with clear surfaces, mirror lenses, and glass lenses. They do not inspect flaws with the attributes of small blemishes on textured LED lenses with uneven surfaces. Consequently, we present a new approach combining wavelet packet transform and partial least squares techniques for flaw inspection on the textured and uneven surfaces of LED lenses.

The wavelet transform allows a time-frequency decomposition of the input signal, but the degree of frequency resolution in the wavelet transform is classically contemplated too coarse for empirical time-frequency analysis [14,15]. The wavelet packet transform provides a computationally efficient alternative with sufficient frequency resolution. In the WPT, the filtering operations are also applied to the detailed coefficients. The result is that wavelet packets provide a sub-band filtering of the input signal into progressively finer equal-width intervals [16]. Kim and Kang [17] used wavelet packet frame and Gaussian mixture model to do texture classification and segmentation. Lee et al. [18] proposed a feature-based adaptive wavelet packet method to inspect surface defect on cold rolled strips.

The partial least squares technique was initially proposed by Wold [19]. It is a statistical multivariate method that finds a regression model by projecting the predicted variables and the observable variables to a new space [20,21]. The PLS finds the latent variables from data sets by capturing the largest variance in the data and achieves the maximum correlation between the predictor variables and response variables [22]. Aznar et al. [23] developed PLS regression models to predict the aged red wine aroma properties from aroma chemical composition. Naganathan et al. [24] implemented a PLS analysis of near-infrared hyperspectral images for beef tenderness prediction. Li et al. [25] applied PLS method to inspection and grading of surface defects of fruits in computer vision fields. Therefore, the PLS method has been successfully applied in diverse fields including process modeling, fault detection, process monitoring and it deals with noisy and highly correlated data, etc., in recent years [26].

3. **Proposed WPLS Approach.**

This study proposes a wavelet packet transformation based partial least squares (WPLS) approach to detect surface defects of textured LED lenses. Five steps are developed to finish the process of flaw detection. Firstly, image preprocessing is executed to remove background region and produce a fused image by integrating the LED lens region with a controlled background to decrease the obstruction of the original background. Secondly, the fused spatial domain image is converted to WPT domain and the wavelet features of the sub-band images are extracted. Thirdly, the suggested PLS method is applied to multivariate transform and data reduction with wavelets features to obtaining latent images. There is as much information in the latent components compared with those in the original features. Fourthly, the latent images are fitted by a regression model to produce a predicted image. Fifthly, the predicted image subtracts with the original image to get the residual image where the surface defects have been separated. Therefore, the visual defects on the uneven surfaces of textured LED lenses can be accurately identified and located by the proposed approach. Figure 3 describes the flow chart of the proposed approach. Figure 4 depicts the data concept diagram of the WPLS approach.

3.1. **Image preprocessing procedure.**

Image preprocessing is first executed to divide two kinds of texture regions where surface defects may happen. ROI (region of interest) is a rectangular block that includes the object(s) to be investigated. The adoption of ROI avoids uninterested regions from obstructing neighborhood computations or frequency analyses. When an image having uninterested regions is transformed into the frequency

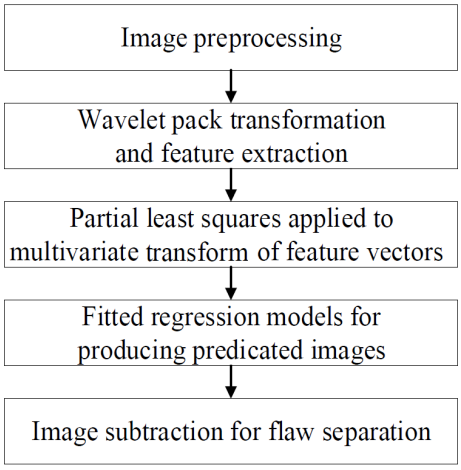

FIGURE 3. Flow chart of the WPLS approach

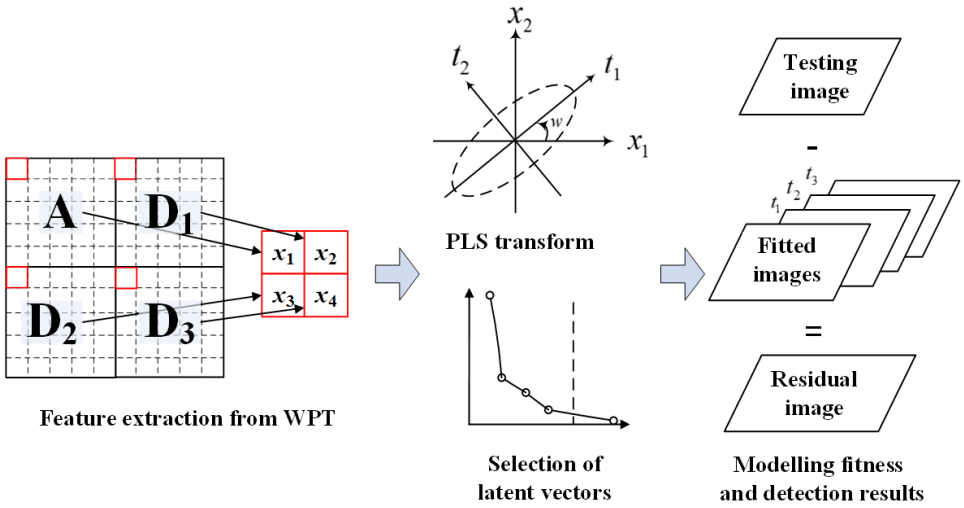

FIGURE 4. Data concept diagram of the WPLS approach

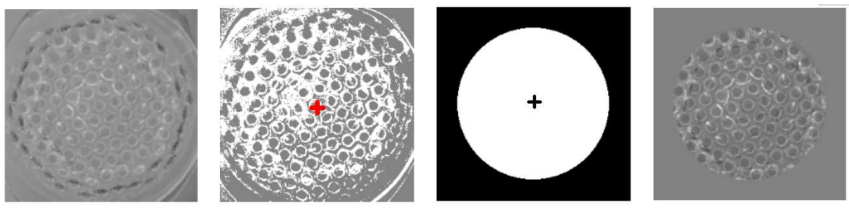

FIGURE 5. The procedure of producing a fused image for the LED lens

domain, the uninterested region (e.g., the background) can notably obstruct the frequency analysis of the object of interest. Therefore, after we capture the image of the target lens and background, we produce a mask to depict the ROI, the region of the target lens. Then, we acquire a fused image by integrating the target region with a controlled background to decrease the obstruction of an uninterested region (the original background). This fused image will then be applied as the input for further wavelet packet transformation.

Figure 5 shows the procedure of producing a fused image for the LED lens. Figure 5(a) is the captured image and Figure 5(b) shows a segmented image with a cross exactly

locating in the mass center of the target lens and the average gray level of the lens region is computed. Figure 5(c) shows the ROI mask of the testing image which can determine the exact region of the target lens. Figure 5(d) shows a fused image produced by integrating the circular lens region into a background that is made up by replicating the average gray level of the lens region in Figure 5(b). With such a controlled background, we not only obtain a rectangular block for wavelet packet transform but also minimize the influence of the non-lens region.

3.2. **Wavelet packet transform.** The inspection task of this study involves detecting unconventional but unclearly flawed items, visual defects on the uneven surfaces of textured LED lenses of optical components. Many of these unexpected blemishes are highly small in size and cannot be described by definite measures, thus making automated defect detection hard. With good time-frequency differentiation capability and flexible time-frequency windows, wavelet transforms are now diffusely adopted for analysis of various signals in time and frequency domain concurrently [16]. In the wavelet decomposition procedure, the general stage breaks the approximated coefficients into two parts. After the dividing, we acquire a vector of approximated coefficients and a vector of detailed coefficients and both of the vectors are at a coarser measure. The information missed between two consecutive approximations is caught in the detailed coefficients. The next stage includes dividing the new approximated coefficient vector; consecutive details are never reexamined. In the relevant wavelet packet circumstance, each detailed coefficient vector is also decomposed into two parts using the same procedure as in approximated vector dividing.

Because of decomposition of only the approximated component at each level, the results of frequency resolution in higher level wavelet decompositions (e.g., A_1 and D_1) are less advisable in a general wavelet analysis. It may lead to problems while employing wavelet transform in some applications which the major information is located in higher frequency components. The frequency resolution of the decomposition filter may not be delicate enough to abstract essential information from the decomposed components of the signal. The required frequency resolution can be accomplished by conducting a wavelet packet transform to decompose a signal further. The wavelet packet transform is a generalization of wavelet decomposition that provides an abundant range of possibilities for signal analysis. Figure 6 shows a wavelet packet decomposition tree at level 3.

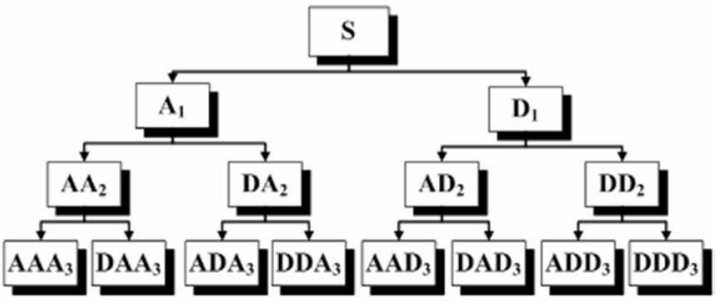

FIGURE 6. Wavelet packet decomposition tree at level 3

One level of wavelet packet decomposition generates one smooth approximated sub-image and three detailed sub-images that have delicate structures with horizontal, vertical, and diagonal orientations. An image is decomposed by wavelet packet transform into one approximated sub-image (A) and three detailed sub-images (D_1, D_2 and D_3). The proposed method extracts the four textural features of one level wavelet packet decomposition to detect surface blemishes of textured LED lenses. The one level wavelet

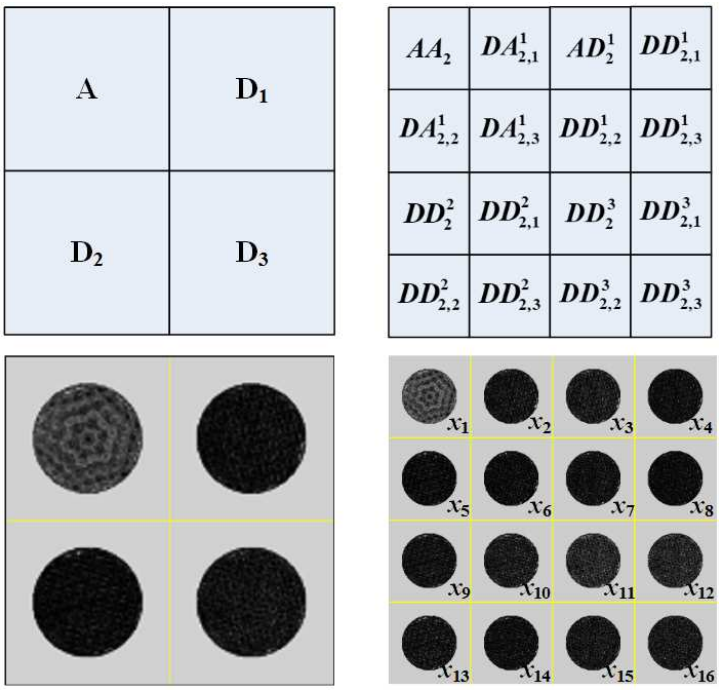

(a) (b)

FIGURE 7. A normal lens image after being processed (a) 1 level and (b) 2 levels of wavelet packet decompositions and the decomposed components with their corresponding variable numbers

packet decomposition is used to precisely locate the pixels with the textural characteristics. Multi-level wavelet decomposition generates coarser expression of the original image. A large number of decomposition levels will result in the fusion effect for the flaws and may cause localization error of the detected defect [7]. Figure 7 shows a normal lens image after being processed 1 and 2 levels of wavelet packet decompositions and the decomposed components with their corresponding variable numbers.

Since WPT has the advantages of being fine enough to extract necessary information from the decomposed components and representing generalization of multi-resolution decomposition, it provides better control of frequency resolution for the decomposition of the signal [16]. Such advantages make WPT suitable and favorable for our study of visual defect detection of textured LED lenses with uneven surfaces. To increase the computational efficiency of WPT, the block WPT is adopted that we divide an image into non-overlapping image blocks of equal size which can be executed WPT individually instead of taking one transform on an entire image.

3.3. **Partial least squares method.** PLS method is one of the primary multivariable statistical techniques to decrease the dimensionality of data, to discover the latent variables from the data by catching the major variance among the data, and reaches the maximum correlation between the predictor variables (X) and response variables (Y) [21]. It is used to discover the essential connections between two matrices (X and Y), and in the meanwhile a latent variable scheme to modelling the covariance structures in these two spaces [22]. The PLS regression is a modern method that integrates features from principal component analysis and multiple regression. It is especially suitable when the matrix of predictors has more variables than observations, and when there is multicollinearity among predicator values [19]. Its goal is to predict a set of dependent variables from a set of independent variables. This prediction is accomplished by abstracting from a set of

orthogonal latent variables with better predictive ability. PLS method has been widely applied in various disciplines such as chemistry [23,26], medicine [27], food [24,25,28], and environmental science [29] where predictive linear modeling is necessary.

When the wavelet packet features of the sub-band images are extracted, the PLS technique is applied to multivariate transform and data reduction with wavelets features to obtaining latent images. The latent components have much more information than those in the original features. Subsequently, the latent images are fitted by a regression model to produce a predicted image and then subtract with the original image to get the residual image where the visual defects have been divided.

In the training process of the proposed PLS method, we use the intensity values of normal images as the response variable. The procedure of PLS method is described as the following steps.

Step 1. Take wavelet pack transform $X_k^J(i,j)$ of a testing image $Y(x,y)$ with J decomposition levels and extract the wavelet feature vectors.

Step 2. Let $h=0$ and $Y(n,1)=u_h(n,1)$

Step 3. Let $X(n,a)=E_h(n,a)$

Step 4. Estimate the vector (w) of the h-th latent vector:

$$w'_h(a,1)=\frac{u'(n,1)\cdot E(n,a)}{u'(n,1)\cdot u(n,1)},\ \text{and normalize } w'_h \text{ to obtain } w'_{norm}(a,1)=\frac{w'_{old}(a,1)}{||w'_{old}(a,1)||}$$

Step 5. Calculate the h-th latent image (t):

$$t_h(n,1)=\frac{E_h(n,a)\cdot w(a,1)}{w'(a,1)\cdot w(a,1)}$$

Step 6. Calculate the wavelet loading matrix (p) of the h-th latent image:

$$p'_h(1,a)=\frac{t'_h(n,1)\cdot E(n,a)}{t'_h(n,1)\cdot t_h(n,1)}$$

Step 7. Calculate the regression coefficients (b) of the h-th latent image:

$$b_h=\frac{t'(n,1)\cdot u(n,1)}{t'(n,1)\cdot t(n,1)}$$

Step 8. Calculate the residuals of the h-th latent image described by the $(h+1)$-th latent image:

$$E_{h+1}(n,a)=E_h(n,a)-t_h(n,1)\cdot p_h(1,a)$$

Step 9. Repeat Step 4 until $h=a$, then stop.

In the above equations, w_h is a latent vector, t_h is a latent image, u_h is a score vector of dependent variable Y, p'_h is a loading vector of variable Y, b_h is a regression coefficient vector, and E_h is a residual image in the h-th iteration. The latent image of the current iteration is obtained from the residual estimate of the previous latent image. These latent vectors are orthogonal each other. Figure 8 shows the matrix decomposition of the PLS method.

The number of PLS dimensions is calculated by percentage of variance explained and cross validation [20]. The cross-validation procedure determines the number of latent variables for obtaining better ability of the model fitness. The index of prediction sum of squares (PRESS) is used to evaluate the model fitness. It is expressed as,

$$PRESS=\sum_{x=0}^{W}\sum_{y=0}^{H}\left[Y(x,y)-\hat{Y}(x,y)\right]^2, \tag{1}$$

where $Y(x, y)$ is the testing image and $\hat{Y}(x, y)$ is the fitted image. Figure 9 shows the PLS fitted images with various numbers of latent vectors and the corresponding resulting images of flaw detection. We find the fitted image with 4 latent vectors has a better flaw detection result of the textured LED lens. Table 1 shows the PLS models with different numbers of latent vectors and their corresponding PRESS indices. The PLS model with 4 latent vectors has the lowest PRESS index for the testing image and obtains a better result of flaw detection.

Figure 10 shows the whole process and the work-in-process results of the proposed WPLS method for detecting surface defects on textured LED lenses. Figure 10(b) presents the WPT domain images of the testing image Figure 10(a). Figure 10(c) is the latent images with various numbers of latent vectors by PLS model. After the latent images

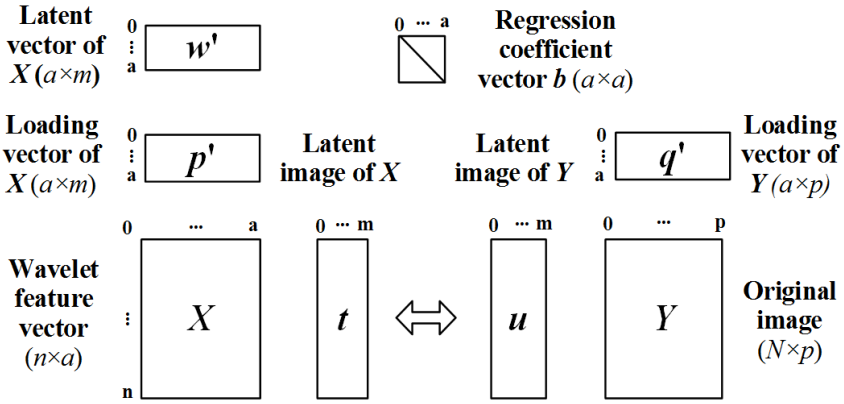

FIGURE 8. Matrix decomposition of PLS method

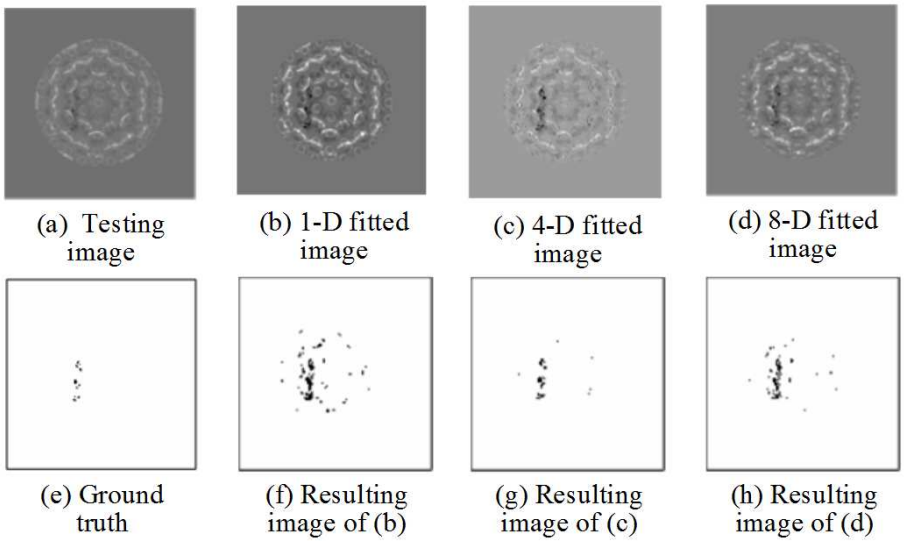

FIGURE 9. Fitted images with various numbers of latent vectors and the corresponding resulting images

TABLE 1. PLS models with different numbers of latent vectors and their PRESS indices

Number of latent vectors	3	4	5	6	7	8
PRESS	149	118*	127	126	122	120

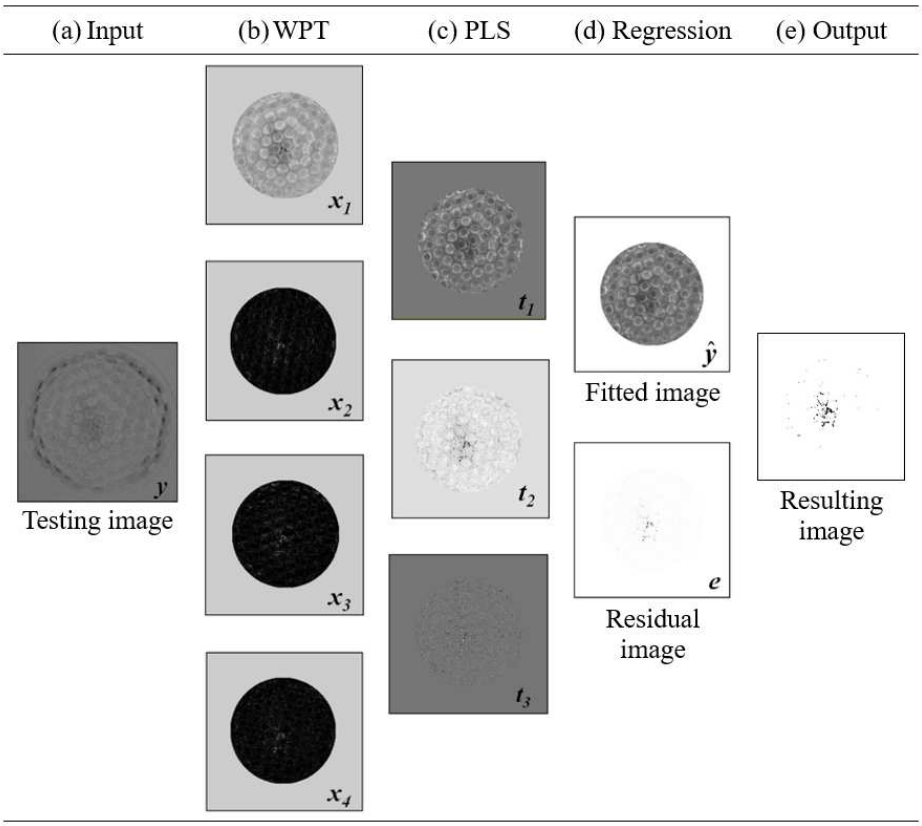

FIGURE 10. The proposed WPLS procedure of detecting visual defects on textured LED lenses: (a) a testing image; (b) the WPT domain images; (c) the latent images of PLS model; (d) the fitted image and residual image; (e) resulting binary image

are fitted by a regression model to produce a fitted image and then subtract with the original image to get the residual image, Figure 10(d) depicts the fitted image and residual image. Figure 10(e) shows the resulting binary images that show the flaws in black by the proposed detection method. The results reveal that the surface flaws on textured lens are correctly separated in the binary image, regardless of LED lens with textured surface.

4. **Implementation and Analyses.** In this section, we implement the proposed approach and conduct experiments to evaluate its performance in detecting visual defects of textured LED lenses. To strengthen the visibility of the visual defects, we make use of the following equipment: a red ring lighting device, a USB 2.0 color CCD of ARTRAY company, a lens with 1 to 10 amplifications of changeable focal lengths, and a XYZ electronic control table with a controller. Experiments are conducted on 320 real textured LED lenses (including 220 normal lenses and 100 defective lenses) provided by a local manufacturing company of high quality LED lenses in Taiwan to evaluate the performance of the proposed approach. Figure 11 demonstrates the configurations of the environment in which we scan real textured LED lenses to be used as testing samples in the experiments. Each image of the LED lens has a size of 512×512 pixels and a gray level of 8 bits. The surface flaw detection algorithm is edited in C language and executed on the 6th version of the C++Builder complier on a personal computer (Pentium-4 2.8 GHz and 512 MB DDRII 667Hz-RAM).

To numerically confirm the manifestation of the proposed method and other approaches, we compare the results of our experiments against those provided by professional

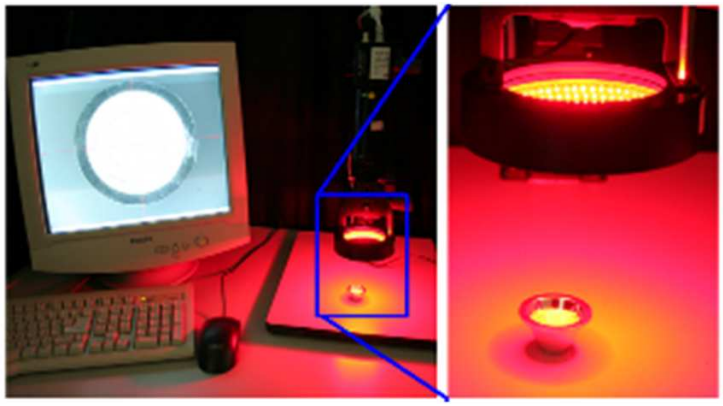

(a) (b)

FIGURE 11. Environmental configurations of scanning a textured LED lens sample: (a) hardware setup of experiments; (b) a textured LED sample is placed under a CCD camera

inspectors. The performance evaluation indices, $(1-\alpha)$ and $(1-\beta)$, are used to represent correct detection judgments; the higher the two indices are, the more accurate the detection results are [30]. Statistical type I error α suggests the probability of producing false alarms, i.e., detecting normal regions as defects. Statistical type II error β implies the probability of producing missing alarms, which fail to alarm real defects. We divide the area of normal region detected as defects by the area of actual normal region to obtain type I error, and the area of undetected defects by the area of actual defects to obtain type II error. The correct classification rate (CR) is defined as:

$$CR = (N_{cc} + N_{dd})/N_{total} \times 100\% \tag{2}$$

where N_{cc} is the pixel number of normal textures detected as normal areas, N_{dd} is the pixel number of defects detected as defective regions, and N_{total} is the total pixel number of a testing image.

4.1. **Performance assessment of distinct detection techniques.** Figure 12 shows partial results of detecting surface flaws by the Otsu method [31], Iterative method [32], Lin and Jiang method [8], Lin and Ho method [6], proposed method, and professional inspector (ground truth), individually. The two spatial domain techniques, the Otsu and Iterative methods, make lots of erroneous judgments (false alarms) on visual defect detection. The three frequency domain techniques, the Lin and Jiang approach, the Lin and Ho approach and the proposed method, detect most of the visual blemishes and make less erroneous judgments. Therefore, the frequency domain approaches outperform the spatial domain techniques in the surface defect detection of textured LED lenses.

Table 2 summarizes the detection results of our experiments. Two spatial domain approaches and two frequency domain techniques are evaluated against the results by professional inspectors. The average defect detection rates $(1-\beta)$ of all testing samples by the five methods are, espectively, 92.00% (Otsu method), 98.50% (Iterative method), 69.30% (Lin and Jiang method), 47.10% (Lin and Ho method), and 93.49% (proposed method). However, the two spatial domain methods have significantly higher false alarm rates (α), 7.90% (Otsu method) and 15.60% (Iterative method). On the contrary, the other two frequency domain approaches have rather lower false alarm rates, 0.08% (Lin and Jiang method), 6.20% (Lin and Ho method) and 0.10% (proposed method). The proposed method has higher correct classification rates (CR) than do the other methods applied to defect detection of textured LED lens images. More specifically, the proposed

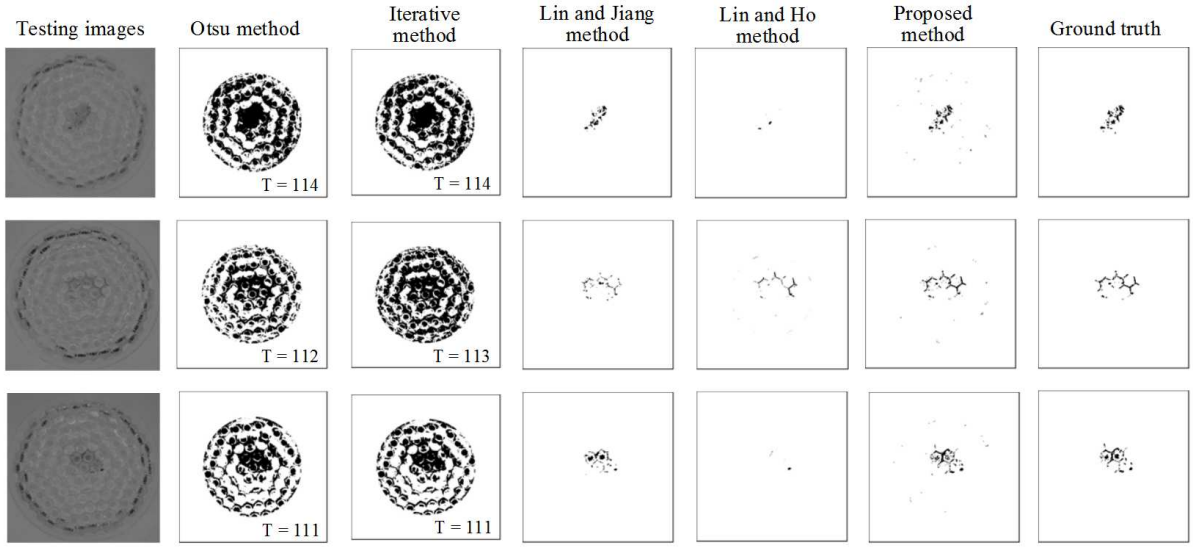

FIGURE 12. Partial detection results of the Otsu method, manual Iterative method, Lin and Jiang method, Lin and Ho method, proposed methods, and inspector (ground truth)

TABLE 2. Summarized comparison table of visual defect detection of textured LED lenses for five different methods

	Spatial domain approaches		Frequency domain approaches		
	Otsu method	Iterative method	Lin and Jiang method	Lin and Ho method	Proposed method
$1-\beta$ (%)	92.00	98.50	69.30	47.10	93.49
α (%)	7.90	15.60	0.08	6.20	0.10
CR (%)	92.10	84.50	99.80	93.50	99.84
Time (s)	0.056	0.054	0.735	1.245	0.113

method not only has a higher detection rate than does the Lin and Jiang method but also its false alarm rate is almost the same as that of the latter method applied to textured LED lens images.

The average computation time for processing an image of 512×512 pixels is as follows: 0.056 seconds by the Otsu method, 0.054 seconds by the Iterative method, 0.735 seconds by the Lin and Jiang method, 1.245 seconds by the Lin and Ho method, and 0.113 seconds by the proposed method. The average processing time of the proposed method is more than six times shorter than that of the Lin and Jiang method. The proposed method overcomes the difficulties of detecting visual blemishes on LED lens images with textured surfaces and excels in its ability of correctly discriminating visual blemishes from normal regions.

4.2. **Performance assessment of WPT based multivariate techniques.** To evaluate the performance of the proposed wavelet packet transform based multivariate approach, experiments with different multivariate techniques are conducted. We compare defect detection results of applying different multivariate methods and analyze their receiver operating characteristic (ROC) curves. The wavelet packet transform is applied to conducting image processing for extracting texture features, because the merits of wavelet packet transform include local image processing, simple calculations, high speed processing and multiple image information. Then, we use three popular multivariate techniques,

PLS, PCA (principal component analysis), and BPN (back propagation network), that integrate multiple texture characteristics to synthesize multiple image features. After image features are incorporated, the decision values are used to judge the existence of defects. This wavelet packet based multivariate techniques are ideally suited for describing locally gradual changes in textured images of LED lenses. Figure 13 demonstrates the partial detection results and erroneous judgements of a testing image by the WPCA, WBPN, and WPLS methods. The suggested WPLS method not only accurately detects most of the real defect regions but also makes less false flaw regions. Table 3 summarizes a comparison table of visual defect detection of textured LED lenses for the three wavelet packet based multivariate techniques in large sample experiments. The time in Table 3 does not include the time (37.4 ms) of processing the same procedure of WPT for the three methods. The proposed WPLS method outperforms the other wavelet packet transform based multivariate techniques in effectiveness indices (false alarm rate, defect detection rate, correct classification rate) as well as efficiency indices (training time, testing time).

Computational complexity is the measure of resources necessary for executing an algorithm in computer science. When the essence of the resources is not definitely given, this is generally the time needed for executing the algorithm. The executing time can also be expressed as the number of needed fundamental operations. To analyze the computational complexity of the PLS method, some major parameters are needed to be set

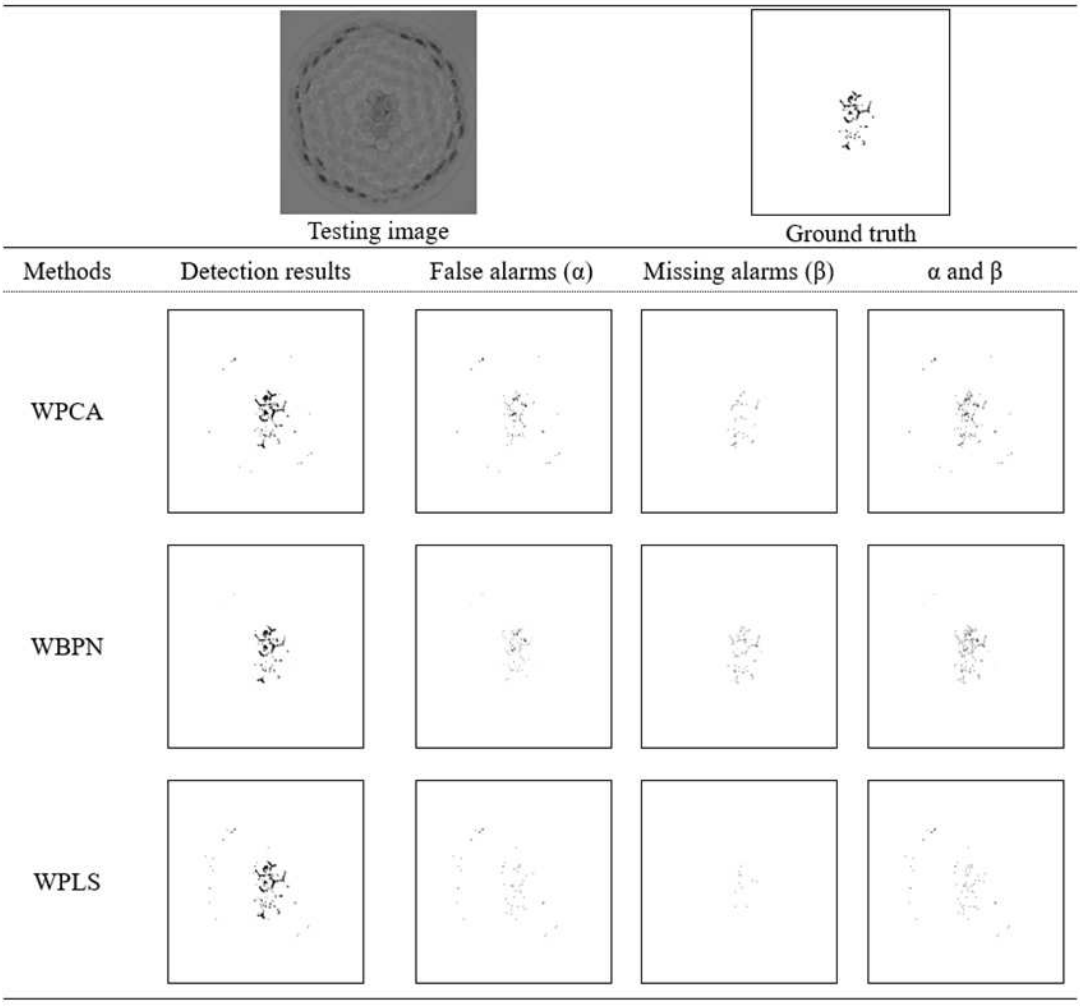

FIGURE 13. Partial detection results and erroneous judgements by the W-PCA, WBPN, and WPLS methods

TABLE 3. Summarized comparison table of visual defect detection of textured LED lenses for three WPT based multivariate techniques

Methods \ Indices	α (%)	$1-\beta$ (%)	CR (%)	Testing time (ms)	Training time (ms)
WPCA	0.220	88.18	99.66	81.09	283
WBPN	0.140	86.78	99.77	200	600,000
WPLS	0.102	93.49	99.84	75.6	237

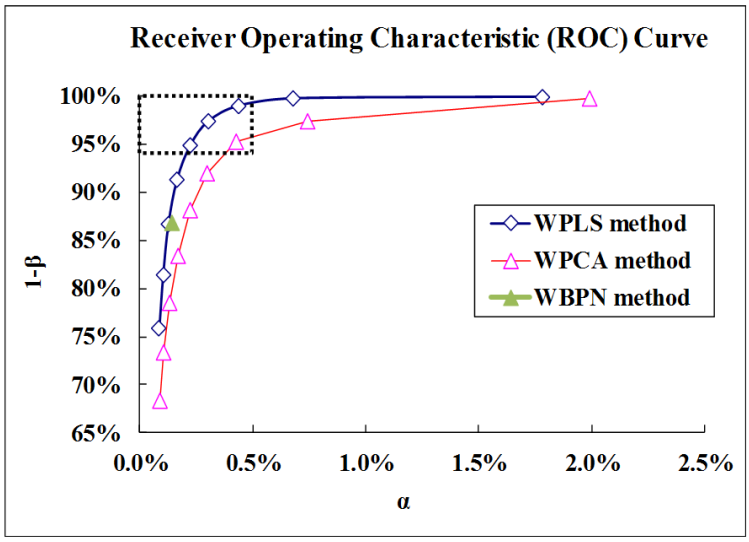

FIGURE 14. ROC curves of the wavelet packet based PCA, BPN and PLS techniques

including the dimensions of latent variables, the maximum iterations when each dimension is solved, the number of sample pairs in the training set, and the number of total categories [33]. The cross validation of the PLS method provides a simple and straightforward stopping rule and makes it simple to compare the estimates of different methods [34]. The PCA method, similar to PLS, projects the input data onto its principal components and performs univariate regressions in these directions. However, the PCA method selects projection solely based on the input distribution and this easily leads to choosing inefficient projections [35]. The BPN method is an iterative technique for learning the relationship between an input and output. This algorithm has been successfully employed in many real-world applications; however, it suffers from slow convergence problems [36]. The main disadvantage of backpropagation is its excessive computational complexity.

For a given hypothesis testing, different decision thresholds lead to different pairs of false alarm rate (α) and detection rate ($1-\beta$) that describe the performance of the statistical test. An ROC curve plots pairs of the specificity (false alarm rate) and the sensitivity (detection rate) as points when various decision thresholds are used. The plot depicts the tradeoff between the sensitivity and specificity. The ROC curve provides a good standard for comparison of detection methods: for a given false alarm probability, the method providing the highest detection probability can be considered the best. Figure 14 shows the ROC curves of the wavelet packet based PCA, BPN, and PLS methods by plotting pairs of the false alarm rate and the detection rate of surface flaw defect detection. The nearer the ROC curve of a test is to the upper-left corner (representing 100% detection rate and 0% false alarm rate), the better the performance of the test is. Since the ROC curve of the WPLS method is nearer to the upper-left corner than those of the WPCA

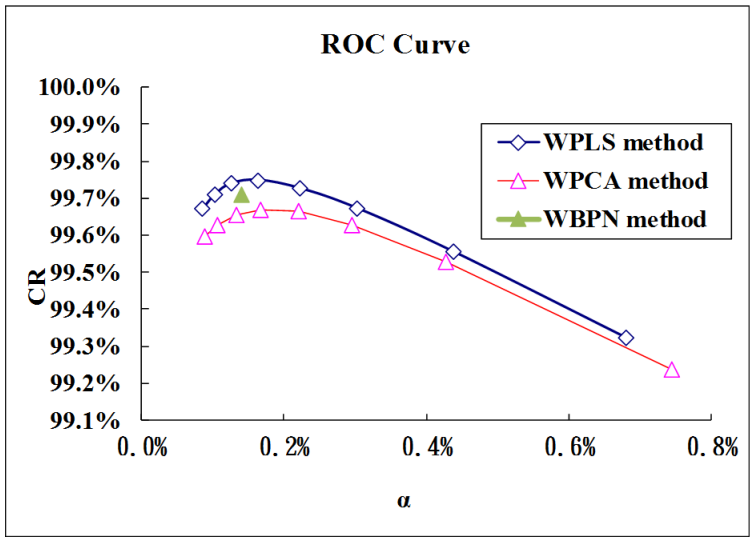

FIGURE 15. Curves of classification rates (CR) v.s. false alarm rates (α) of the wavelet packet based PCA, BPN and PLS techniques

and the WBPN methods, the WPLS method performs better than the WPCA and the WBPN methods in appearance flaw detection of LED lenses with respect to both the false alarm rate and the detection rate.

Figure 15 compares the three wavelet packet based techniques at various false alarm rates, when the classification rates (CR), instead of the detection rates ($1 - \beta$), is the subject of interest. All of the three techniques can achieve a CR value of more than 99.5%, when the false alarm rate approaches to 0.02. If we compare the performance at the same false alarm rate, the WPLS method outperforms the WPCA and the WBPN methods in overall situation.

5. **Conclusions.** Machine vision technologies improve product quality and production productivity, and provide competitive advantages to industries that employ these techniques. This study proposes a wavelet packet transformation based partial least squares approach for the automatic inspection of visual defects on textured and uneven surfaces of LED lenses. Real textured LED lenses are used as testing samples, and large-sample experiments are conducted in a practical inspection environment to verify the performance of the proposed approach. Experimental results show that the proposed method achieves a high 93.49% probability of correctly discriminating visual defects from normal regions and a low 0.10% probability of erroneously detecting normal regions as defects on textured surfaces of LED lenses. Compared with other wavelet packet based multivariate techniques, the proposed WPLS method has the advantages of higher detection rates, lower false alarm rates, and shorter average processing time than those of the WPCA and WBPN models. This research contributes a solution to a common visual defect detection problem of textured LED lenses and offers a computer-aided surface defect inspection system to meet the inspection and quality control request. Future research may extend the proposed approach to determine the concentration levels of the surface flaws (e.g., very serious, serious, moderately serious, and minor) and employ the proposed techniques to inspect transparent LED lenses with distinct surface flaws.

Acknowledgment. The authors thank the Ministry of Science and Technology, Taiwan, for the financial support through the Grant MOST 104-2221-E-324-010.

REFERENCES

[1] H.-D. Lin and Y.-S. P. Chiu, RBF network and EPC method applied to automated process regulations for passive components dicing, *International Journal of Innovative Computing, Information and Control*, vol.6, no.11, pp.5077-5091, 2010.

[2] H.-D. Lin, Y.-S. P. Chiu and W.-T. Lin, An innovative approach for detection of slight surface variations on capacitor chips, *International Journal of Innovative Computing, Information and Control*, vol.9, no.5, pp.1835-1850, 2013.

[3] H.-D. Lin and K.-S. Hsieh, Detection of surface variations on curved mirrors of vehicles using slight deviation control techniques, *International Journal of Innovative Computing, Information and Control*, vol.14, no.4, pp.1407-1421, 2018.

[4] F. Adamo, F. Attivissimo, A. D. Nisio and M. Savino, A low-cost inspection system for online defects assessment in satin glass, *Measurement*, vol.42, pp.1304-1311, 2009.

[5] H. Liu, Y. Wang and F. Duan, Glass bottle inspector based on machine vision, *International Journal of Computer Systems Science and Engineering*, vol.3, no.3, pp.162-167, 2008.

[6] H. D. Lin and D. C. Ho, Detection of pinhole defects on chips and wafers using DCT enhancement in computer vision system, *International Journal of Advanced Manufacturing Technology*, vol.34, nos.5-6, pp.567-583, 2007.

[7] W. C. Li and D. M. Tsai, Wavelet-based defect detection in solar wafer images with inhomogeneous texture, *Pattern Recognition*, vol.45, pp.742-756, 2012.

[8] H. D. Lin and J. D. Jiang, Applying discrete cosine transform and grey relational analysis to surface defect detection of LED, *Journal of the Chinese Institute of Industrial Engineers*, vol.24, no.6, pp.458-467, 2007.

[9] Y. P. Chiu and H. D. Lin, An innovative blemish detection system for curved LED lenses, *Expert Systems with Applications*, vol.40, no.2, pp.471-479, 2013.

[10] M. Rebsamen, J. M. Boucheix and M. Fayol, Quality control in the optical industry: From a work analysis of lens inspection to a training programme, an experimental case study, *Applied Ergonomics*, vol.41, pp.150-160, 2010.

[11] S. S. Martínez, J. G. Ortega, J. G. García and A. S. García, A sensor planning system for automated headlamp lens inspection, *Expert Systems with Applications*, vol.36, pp.8768-8777, 2009.

[12] A. I. Bazin, T. Cole, B. Kett and M. S. Nixon, An automated system for contact lens inspection, *Lecture Notes in Computer Science*, vol.4291, pp.141-150, 2006.

[13] D. B. Perng, W. C. Wang and S. H. Chen, A novel quasi-contact lens auto-inspection system, *Journal of the Chinese Institute of Industrial Engineers*, vol.27, no.4, pp.260-269, 2010.

[14] S. G. Mallat, A theory for multiresolution signal decomposition the wavelet representation, *IEEE Trans. Pattern Analysis and Machine Intelligence*, vol.11, no.7, pp.674-693, 1989.

[15] S. G. Mallat, Multifrequency channel decompositions of image and wavelet models, *IEEE Trans. Acoustics, Speech, and Signal Processing*, vol.37, no.12, pp.2091-2110, 1989.

[16] G. G. Amiri and A. Asadi, Comparison of different methods of wavelet and wavelet packet transform in processing ground motion records, *International Journal of Civil Engineering*, vol.7, no.4, pp.248-257, 2009.

[17] S. C. Kim and T. J. Kang, Texture classification and segmentation using wavelet packet frame and Gaussian mixture model, *Pattern Recognition*, vol.40, pp.1207-1221, 2007.

[18] C. S. Lee, C. H. Choi, J. Y. Choi and S. H. Choi, Surface defect inspection of cold rolled strips with features based on adaptive wavelet packets, *IEICE Trans. Information and Systems*, vol.E80-D, no.5, pp.594-604, 1997.

[19] H. Wold, Estimation of principal components and related models by iterative least squares, in *Multivariate Analysis II*, P. R. Krishnaiah (ed.), New York, Academic Press, 1966.

[20] P. Geladi and B. R. Kowalski, Partial least squares regression: A tutorial, *Analytica Chimica Acta*, vol.185, pp.1-17, 1986.

[21] I. S. Helland, Partial least squares regression and statistical models, *Scandinavian Journal of Statistic*, vol.17, pp.97-114, 1990.

[22] H. Martens and T. Naes, *Multivariate Calibration*, 2nd Edition, Wiley's Publisher, Chichester, 1992.

[23] M. Aznar, R. López, J. Cacho and V. Ferreira, Prediction of aged red wine aroma properties from aroma chemical composition. Partial least squares regression models, *Journal of Agricultural and Food Chemistry*, vol.51, no.9, pp.2700-2707, 2003.

[24] G. K. Naganathan, L. M. Grimes and J. Subbiah, Partial least squares analysis of near-infrared hyperspectral images for beef tenderness prediction, *Sensing and Instrumentation for Food Quality and Safety*, vol.2, no.3, pp.178-188, 2008.

[25] J. Li, X. Rao and Y. Ying, Inspection and grading of surface defects of fruits by computer vision, *Advanced Materials Research*, vols.317-319, pp.956-961, 2011.

[26] R. M. Correia, E. Domingos, F. Tosato, L. F. M. Aquino, A. M. Fontes, V. M. Cáo, P. R. Filgueiras and W. Romão, Banknote analysis by portable near infrared spectroscopy, *Forensic Chemistry*, vol.8, pp.57-63, 2018.

[27] L. Khedher, J. Ramírez, J. M. Górriz, A. Brahim and F. Segovia, Early diagnosis of Alzheimer's disease based on partial least squares, principal component analysis and support vector machine using segmented MRI images, *Neurocomputing*, vol.151, no.1, pp.139-150, 2015.

[28] Y.-Z. Feng, G. ElMasry, D.-W. Sun, A. G. M. Scannell, D. Walsh and N. Morcy, Near-infrared hyperspectral imaging and partial least squares regression for rapid and reagentless determination of Enterobacteriaceae on chicken fillets, *Food Chemistry*, vol.138, pp.1829-1836, 2013.

[29] A. M. Mouazen, B. Kuang, J. D. Baerdemaeker and H. Ramon, Comparison among principal component, partial least squares and back propagation neural network analyses for accuracy of measurement of selected soil properties with visible and near infrared spectroscopy, *Geoderma*, vol.158, no.1, pp.23-31, 2010.

[30] D. C. Montgomery and G. C. Runger, *Applied Statistics and Probability for Engineers*, 4th Edition, John Wiley & Sons, NJ, USA, 2007.

[31] N. Otsu, A threshold selection method from gray level histogram, *IEEE Trans. Systems, Man and Cybernetics*, vol.9, pp.62-66, 1979.

[32] R. Jain, R. Kasturi and B. G. Schunck, *Machine Vision*, International Editions, McGraw Hill, New York, 1995.

[33] J. He, B. Ma, S. Wang, Y. Liu and Q. Huang, Cross-modal retrieval by real label partial least squares, *Proc. of the 2016 ACM on Multimedia Conference*, pp.227-231, 2016.

[34] S. Wold, A. Ruhe, H. Wold and W. J. Dunn III, The collinearity problem in linear regression. The partial least squares (PLS) approach to generalized inverses, *SIAM Journal on Scientific and Statistical Computing*, vol.5, no.3, pp.735-743, 1984.

[35] S. Vijayakumar and S. Schaal, Locally weighted projection regression: An $O(n)$ algorithm for incremental real time learning in high dimensional space, *Proc. of the 17th International Conference on Machine Learning*, pp.1079-1086, 2000.

[36] Z. Yan, S.-Y. Cho and S. W. Shaker, Predictive block-matching algorithm for wireless video sensor network using neural network, *Journal of Computer and Communications*, vol.5, pp.66-77, 2017.